Oncogene (2005) 24, 6719–6728

www.nature.com/onc

Activated AKT regulates NF-κB activation, p53 inhibition and cell survival in HTLV-1-transformed cells

Soo-Jin Jeong[1], Cynthia A Pise-Masison[1], Michael F Radonovich[1], Hyeon Ung Park and John N Brady*[,1]

[1]*Virus Tumor Biology Section, Laboratory of Cellular Oncology, Center for Cancer Research, National Cancer Institute, National Institutes of Health, Bethesda, MD 20892-5055, USA*

AKT activation enhances resistance to apoptosis and induces cell survival signaling through multiple downstream pathways. We now present evidence that AKT is activated in HTLV-1-transformed cells and that Tax activation of AKT is linked to NF-κB activation, p53 inhibition and cell survival. Overexpression of AKT wild type (WT), but not a kinase dead (KD) mutant, resulted in increased Tax-mediated NF-κB activation. Blocking AKT with the PI3K/AKT inhibitor LY294002 or AKT SiRNA prevented NF-κB activation and inhibition of p53. Treatment of C81 cells with LY294002 resulted in an increase in the p53-responsive gene *MDM2*, suggesting a role for AKT in the Tax-mediated regulation of p53 transcriptional activity. Further, we show that LY294002 treatment of C81 cells abrogates *in vitro* IKKβ phosphorylation of p65 and causes a reduction of p65 Ser-536 phosphorylation *in vivo*, steps critical to p53 inhibition. Interestingly, blockage of AKT function did not affect IKKβ phosphorylation of IκBα *in vitro* suggesting selective activity of AKT on the IKKβ complex. Finally, AKT prosurvival function in HTLV-1-transformed cells is linked to expression of Bcl-xL. We suggest that AKT plays a role in the activation of prosurvival pathways in HTLV-1-transformed cells, possibly through NF-κB activation and inhibition of p53 transcription activity.
Oncogene (2005) **24,** 6719–6728. doi:10.1038/sj.onc.1208825; published online 20 June 2005

Keywords: HTLV-1; p53; NF-κB; AKT; p65; IKK

Introduction

AKT was identified as a cellular homologue (*c-AKT*) of the viral oncogene (*v-AKT*) from the acutely transforming retrovirus AKT8, isolated from a murine T-cell lymphoma (Staal *et al*., 1977; Bellacosa *et al*., 1991). AKT is also known as protein kinase B (PKB) and its activation can be mediated by the activation of phosphoinositide 3-OH kinase (PI3K) (Dudek *et al*., 1997; Kauffmann-Zeh *et al*., 1997; Kulik *et al*., 1997; Songyang *et al*., 1997). Activation of the PI3K/AKT pathway has been associated with malignant transformation and antiapoptotic signaling. Recently, several targets of the PI3K/AKT pathway have been identified which contribute to its promotion of cell survival. Among these are BAD, caspase 9, the forkhead family, and the NF-κB transcription factor (Thompson and Thompson, 2004). AKT can promote the activation of NF-κB by phosphorylation of IκB kinase (IKK), which in turn, augments the transcriptional activity of NF-κB p65/RelA (Ozes *et al*., 1999). NF-κB can induce cell survival through promotion of antiapoptotic gene expression and inhibition of p53 activity (Mayo and Donner, 2002).

The tumor suppressor p53 protein regulates the response of mammalian cells to stress and DNA damage through transcriptional activation of genes and induces cell cycle arrest, DNA repair, apoptosis, senescence and angiogenesis (Levine, 1997; Sherr, 1998). The role of p53 in the transactivation and transrepression of genes is well established (Slee *et al*., 2004). p53 is able to target the expression of genes including *MDM2*, *p21*, *BAX*, *PIG3*, *PUMA* and *NOXA* whose promoters contain p53-binding sites (Vousden and Lu, 2002). p53 also functions as an inhibitor of cell growth, by inducing cell cycle arrest or apoptotic cell death (Vousden, 2000).

Human T-cell lymphotrophic virus type 1 (HTLV-1) is the etiologic agent of adult T-cell leukemia (ATL) (Poiesz *et al*., 1980; Yoshida *et al*., 1982) and also is involved in chronic inflammatory diseases such as HTLV-1-associated myelopathy/tropical spastic paraparesis (HAM/TSP) (Gessain *et al*., 1985; Osame *et al*., 1986), HTLV-1-associated arthropathy (Nishioka *et al*., 1989), uveitis (Mochizuki *et al*., 1992) and Sjögren's syndrome (Vernant *et al*., 1988). HTLV-1 encodes a 40 kDa protein, Tax, which is critical for viral replication, transformation and gene regulation (Nerenberg *et al*., 1987; Grassmann *et al*., 1989; Tanaka *et al*., 1990; Akagi *et al*., 1995).

We previously demonstrated that HTLV-1 Tax inhibits p53 transcriptional activity and that the NF-κB p65 subunit plays a critical role in Tax-mediated

*Correspondence: JN Brady, Virus Tumor Biology Section, Laboratory of Cellular Oncology, Center for Cancer Research, National Cancer Institute, National Institutes of Health, Building 41/B201, 9000 Rockville Pike, Bethesda, MD 20892-5055, USA;
E-mail: bradyj@exchange.nih.gov
Received 17 March 2005; revised 4 May 2005; accepted 4 May 2005; published online 20 June 2005

p53 inhibition (Pise-Masison *et al*., 2000; Jeong *et al*., 2004). Furthermore, we demonstrated that Tax inhibition of p53 depends upon phosphorylation of p65 at Ser-536 by the upstream kinase IKKβ (Jeong *et al*., 2005). In this study, we investigated whether AKT, which is an upstream kinase of IKKβ, plays a role in the inhibition of p53 by Tax. Our results demonstrated that Tax inhibition of p53 was impaired by overexpression of an AKT kinase dead (KD) mutant or blocking AKT with the PI3K/AKT inhibitor LY294002 or AKT SiRNA. The increase of p53-responsive MDM2 gene expression by LY294002 indicated a direct role for AKT in the regulation of p53 transcription. Tax activation of AKT is linked to IKKβ and p65 phosphorylation. Finally, we demonstrated that blocking AKT by LY294002 induced apoptotic cell death and decreased the level of the antiapoptotic Bcl-xL expression in HTLV-1-transformed cells. This study provides the first evidence that AKT is important for Tax-mediated p53 inhibition and plays a role in protecting HTLV-1-transformed cells against apoptosis.

Results

Tax activates the prosurvival kinase AKT

In previous studies, we have demonstrated that Tax inhibition of p53 function involves the IKKβ and p65 subunit of NF-κB (Jeong *et al*., 2005). In the light of the strong link between AKT and IKKβ activation, we sought to determine if Tax regulated AKT activity. Increasing amounts of Tax plasmid were transfected into 293T cells and activation of AKT was assayed by Western blot analysis of the phosphorylation state of AKT. As seen in Figure 1, expression of Tax resulted in an increased phosphorylation of AKT at Ser-473 and Thr-308. The overall level of AKT remained constant, suggesting that Tax induced the phosphorylation of AKT. This is consistent with a previous report that Tax activates the PI3K pathway and AKT phosphorylation at Ser-473 in long-term Tax-expressing cell lines (Liu *et al*., 2001). The levels of actin were equivalent in all the samples, indicating that an equal amount of protein was loaded in each lane. Importantly, phospho-AKT is found in HTLV-1-transformed cells (see below, Figure 5).

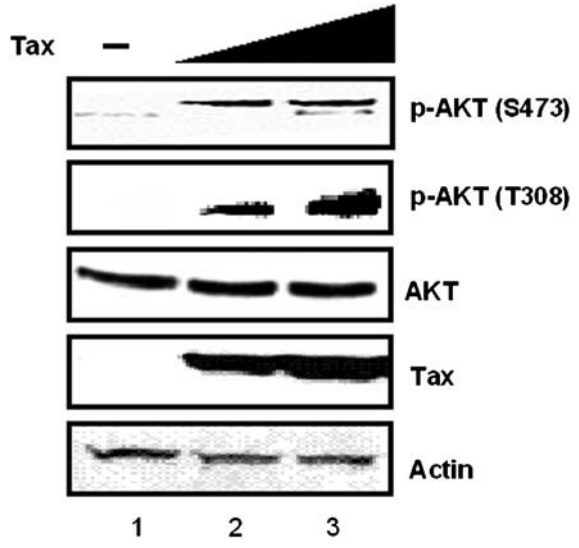

Figure 1 HTLV-1 Tax induces the phosphorylation of AKT. 293T cells were transfected in 100-mm dishes using Effectene reagent (Qiagen) with pcTax (0, 1 or 2 μg) for 48 h. Western blot analysis for phospho-AKT Ser-473, Thr-308 (Cell Signaling), AKT (Upstate), Tax (Tab172) and actin (Santa Cruz) from transfected cells, was performed

AKT is required for Tax-mediated NF-κB activation and p53 inhibition

To investigate whether AKT is involved in Tax inhibition of p53, AKT wild type (WT) or KD was overexpressed along with p53 in Jurkat T lymphocytes in the absence or presence of Tax. Cells were maintained for 24 h after transfection, cell lysates were prepared and luciferase activities were measured for p53-responsive MDM2-Luc. As shown in Figure 2a, p53 activity was inhibited approximately 60% when Tax was cotransfected along with p53 (lanes 3 and 4). Overexpression of AKT WT further increased the level of p53 inhibition in the presence of Tax (lanes 3–6). In contrast, overexpression of AKT KD decreased the level of p53 inhibition in the presence of Tax (lanes 3, 4, 7 and 8).

AKT can promote the activation of NF-κB by phosphorylation of IKKα or β and augmenting the transcriptional activity of NF-κB p65 (Ozes *et al*., 1999; Sizemore *et al*., 1999). To determine if AKT played a role in Tax activation of NF-κB, AKT WT or KD expression plasmids were cotransfected with a Tax expression plasmid and the NF-κB-responsive reporter construct ($4\times$ NF-κB-Luc) into Jurkat lymphocytes. The results of this experiment demonstrated that Tax activated NF-κB activity approximately five-fold. Overexpression of AKT WT increased Tax transactivation to 12-fold. In contrast, overexpression of the AKT KD mutant did not increase Tax transactivation (Figure 2b, lane 6). Since Jurkat T-cells express a relatively high level of phospho-AKT (Shan *et al*., 2000), the AKT KD mutant did not have an inhibitory effect.

Western blot analysis was performed to detect the expression of p53 and AKT (Figure 2c). The result demonstrated that the cells contained equivalent levels of p53. The level of AKT showed a slight increase when AKT WT or KD was overexpressed. As a result of low transfection efficiency of Jurkat cells, we could not detect Tax protein expression by Western blot analysis.

PI3K/AKT inhibitor LY294002 decreases Tax-mediated p53 inhibition

To confirm the importance of AKT in NF-κB activation and p53 inhibition, we used the PI3K inhibitor LY294002 to block the activation of AKT. MEF p65−/− cells were pretreated with LY294002 one hour before transfection and p65 was transfected with or without Tax. At 24 h post-transfection, cell lysates were

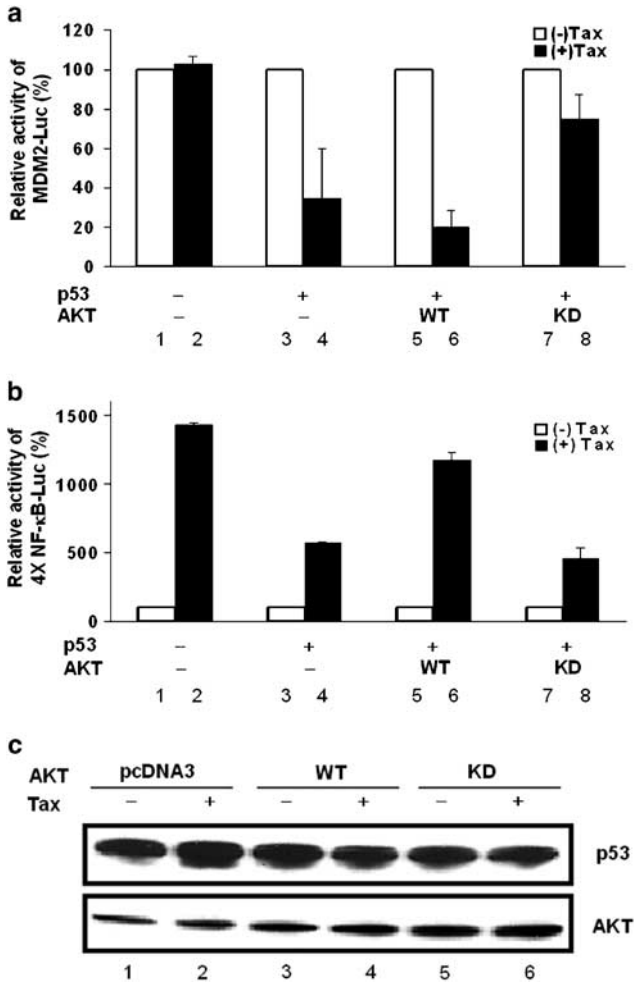

Figure 2 Overexpression of AKT kinase dead (KD) mutant rescues Tax-mediated p53 inhibition. (**a**) Jurkat cells were transfected using Superfect transfection reagent (Qiagen) with reporter constructs (1.0 μg) MDM2-Luc, AKT WT or KD (1.0 μg) and p53 (0.4 μg) in the absence (white) or presence (black) of Tax (2.0 μg). Cells were harvested 24 h after transfection and luciferase activities were measured. Luciferase values were adjusted for transfection efficiency using RSV β-galactosidase. (**b**) Jurkat cells were transfected using Superfect transfection reagent (Qiagen) with reporter constructs (1.0 μg) 4 $\times$ NF-κB-Luc, AKT WT or KD (1.0 μg) and p53 (0.4 μg) in the absence (white) or presence (black) of Tax (2.0 μg). Cells were harvested 24 h after transfection and luciferase activities were measured. Luciferase values were adjusted for transfection efficiency using RSV β-galactosidase. The graph represents the luciferase activity from three independent experiments. The s.d. for the three experiments is included. (**c**) Western blot analyses of transfected cells were performed for p53 (DO-1, Oncogene) and AKT (Upstate)

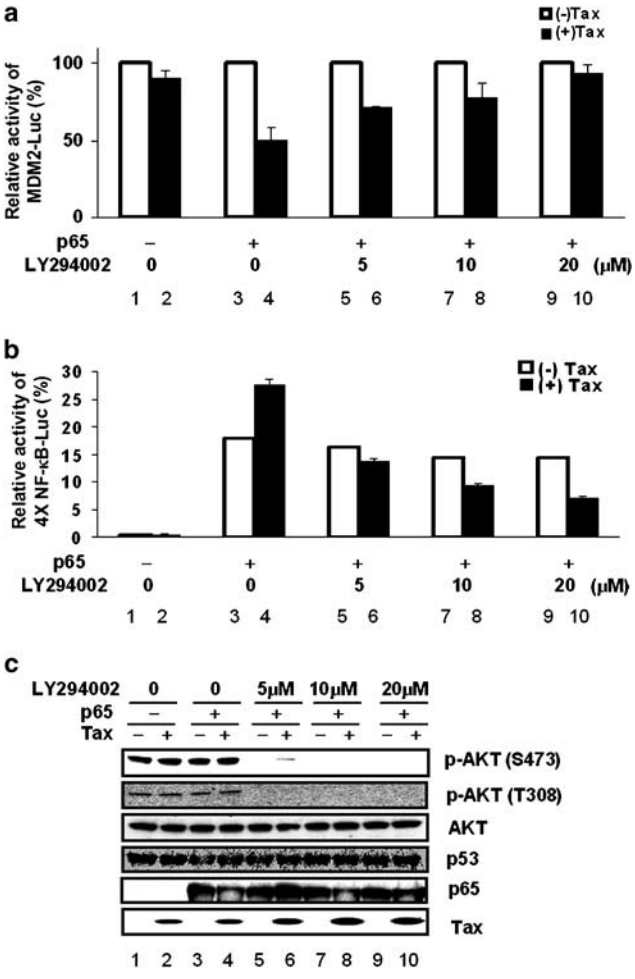

Figure 3 PI3K/AKT inhibitor LY294002 prevents Tax-mediated p53 inhibition. (**a** and **b**) Mouse embryo fibroblast p65−/− cells were transiently transfected using Lipofectamine plus reagent (Invitrogen) with reporter constructs (0.2 μg) MDM2- (**a**) or 4 $\times$ NF-κB-Luc (**b**) and p65 WT (0.05 μg) in the absence (white) or presence (black) of Tax (0.2 μg). LY294002 (5, 10 or 20 μM) was treated 1 h prior to transfection, cells were harvested 24 h after transfection and luciferase activities were measured. Luciferase values were adjusted for transfection efficiency using RSV β-galactosidase. The graph represents the luciferase activity from three independent experiments. The s.d. for the three experiments is included. (**c**) Western blot analysis for phospho-AKT Ser-473 and Thr-308 (Cell Signaling), AKT (Upstate), p65 (CT, Upstate), p53 (Ab1, Oncogene) and Tax (Tab172) from transfected cells, was performed

prepared and luciferase activities were measured for MDM2-Luc and 4 $\times$ NF-κB-Luc. In the presence of a limiting amount of Tax protein, p53 activity was inhibited approximately 50% (Figure 3a, lanes 3 and 4). With increasing concentration of LY294002, the level of p53 inhibition was decreased (Figure 3a, lanes 5–10). At the highest concentration of LY294002 tested, there was no inhibition of p53 activity in the presence of Tax and p65.

LY294002 treatment also decreased Tax-mediated NF-κB activation (Figure 3b, lanes 4, 6, 8 and 10). Transfection of p65 into the p65−/− cells increased NF-κB reporter activity by 54-fold. The addition of Tax further increased NF-κB activity to a 78-fold increase in activity over basal levels. The addition of LY294002 had a modest effect on NF-κB activation by p65 alone (Figure 3b, lanes 3, 5, 7 and 9). At the highest concentration of LY294002, less than a 20% decrease

in NF-κB activity was observed. Of interest, when LY294002 was added to the Tax-expressing cells, a 75% reduction in NF-κB activity was observed (Figure 3b, lanes 4 and 10). These results suggest that AKT is a critical part of the Tax/NF-κB activation cascade. A similar result was observed with the PI3K/AKT inhibitor wortmannin (data not shown).

Western blot analysis was performed to analyse the expression of phospho-AKT, AKT, p53, p65 and Tax in the transfected cells (Figure 3c). As expected, the level of phospho-AKT at Ser-473 and Thr-308 decreased by the treatment with LY294002 (panels 1 and 2). Owing to the high endogenous level of phospho-AKT and/or transfection efficiency of the p65−/− MEFs, an increase in the level of phospho-AKT was not observed in the presence of Tax. The expression of total AKT remained constant (panel 3). The results presented in Figure 3c further demonstrate that there was no significant decrease in the expression of p65 or Tax in the presence of LY294002 (panels 4 and 5). In fact, the level of Tax protein appeared to increase slightly in the treated cells. Thus, the increase in p53 activity does not appear to be due to a change in protein expression.

To investigate the specificity of the kinase inhibition and its effect on NF-κB activation and p53 inhibition, a parallel experiment was carried out with the ERK1/2 kinase inhibitor PD98059, p38 MAPK inhibitor SB203580, PKA inhibitor H-89 and casein kinase (CK) II inhibitor apigenin. Similar to the above experiment, kinase inhibitors were added 1 h prior to transfection of p65 WT, MDM2-Luc and Tax. At 24 h post-transfection, luciferase activities were measured. Unlike LY294002 treatment, the treatment with all other kinase inhibitors did not reverse the Tax-mediated p53 inhibition (data not shown). These results indicate that the PI3K/AKT pathway is involved in the Tax-mediated p53 inhibition pathway.

AKT SiRNA decreases ability of Tax to inhibit p53

In the following experiments, we utilized SiRNA to specifically inhibit AKT. AKT SiRNA was transfected into p65−/− MEFs 12 h prior to transfection of DNAs encoding p65, Tax and MDM2-Luc. As shown in Figure 4a, Tax inhibited p53 activity by approximately 70% in the presence of p65 (lanes 3 and 4). AKT SiRNA transfection rescued p53 activity in the presence of Tax. At the highest concentration of SiRNA tested, 200 nM, there was no Tax-dependent inhibition of p53 (Figure 4a, lanes 7 and 8). We also observed that the AKT SiRNA inhibited the ability of Tax to activate NF-κB (Figure 4b, lanes 7 and 8). AKT SiRNA inhibited p65-mediated NF-κB activation, suggesting that AKT is a part of both the basal and Tax-activated NF-κB pathway.

To demonstrate the specificity of the AKT SiRNA, CAT SiRNA was used as a negative control. The results presented in Figure 4c demonstrated that AKT SiRNA, but not CAT SiRNA, impaired Tax inhibition of p53. The specificity of the inhibition is also demonstrated by Western blot analysis (Figure 4d). The AKT SiRNA, but not the control CAT SiRNA, decreased the level of AKT protein in the cell. Together, the results provide strong evidence that AKT plays an important role in Tax-mediated p53 inhibition.

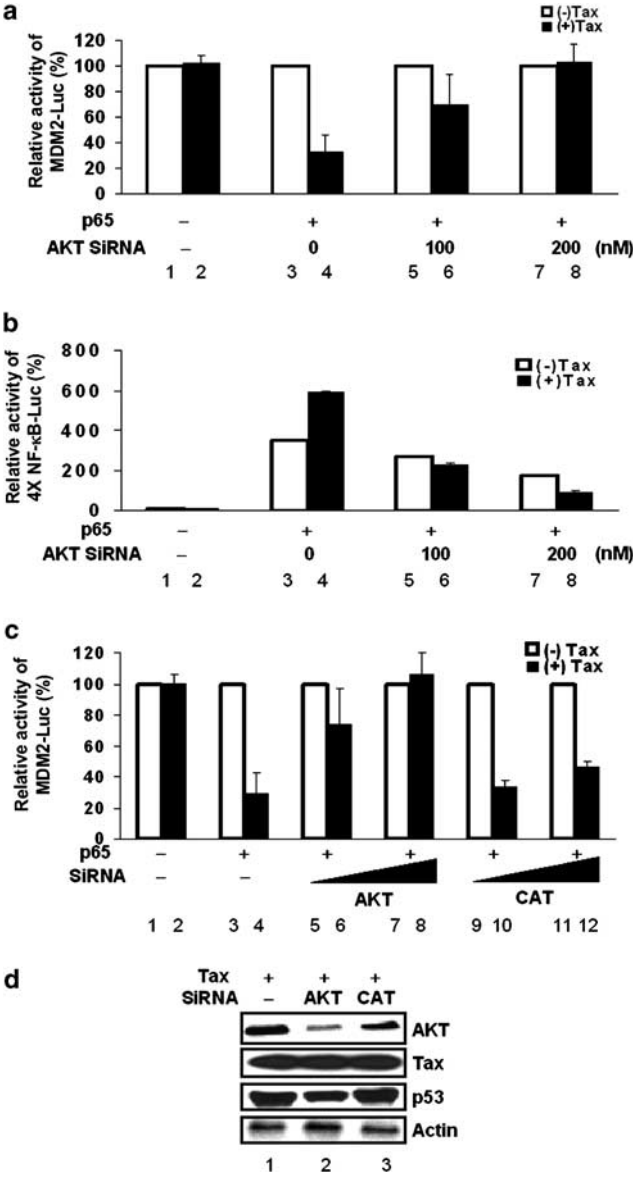

Figure 4 Blocking endogenous AKT by AKT SiRNA prevents Tax-mediated p53 inhibition. (**a** and **b**) SiRNA (100 or 200 nM) for AKT (Dharmacon) was transfected using RNAifect reagent (Qiagen) into mouse embryo fibroblast p65−/− cells. After 12 h, cells were transiently transfected using Lipofectamine plus reagent (Invitrogen) with reporter constructs (0.2 μg) MDM2- (**a**) or 4 × NF-κB-Luc (**b**) and p65 WT (0.05 μg) in the absence (white) or presence (black) of Tax (0.2 μg) for 24 h. Cells were harvested 24 h after transfection and luciferase activities were measured. Luciferase values were adjusted for transfection efficiency using RSV β-galactosidase. The graph represents the luciferase activity from three independent experiments. The s.d. for the three experiments is included. (**c**) To test the specificity of AKT SiRNA, chloroamphenicol acetyltransferase (CAT) SiRNA was utilized as a negative control. Transfection was performed as described above for MDM2-Luc. (**d**) Western blot analysis for AKT, Tax, p53 and actin from transfected cells, was performed. Inhibition of AKT expression is shown in top panel

AKT induces IKKβ kinase activity to phosphorylate p65 in HTLV-1-transformed cells in vitro *and* in vivo

To determine if the AKT pathway was activated in HTLV-1-transformed cells and to determine if AKT contributes to NF-κB activation and p53 inhibition, C81 cells were treated with LY294002 and cell extracts were prepared for Western blot analysis. The results presented in Figure 5a demonstrated that AKT is phosphorylated at Ser-473 and Thr-308 in C81 cells (panels 1 and 2). Treatment with LY294002 decreased phosphorylation at both sites. In parallel, a decrease in p65 phosphorylation at Ser-536 was observed (panel 4), suggesting that AKT is linked to p65 phosphorylation in HTLV-1-transformed cells.

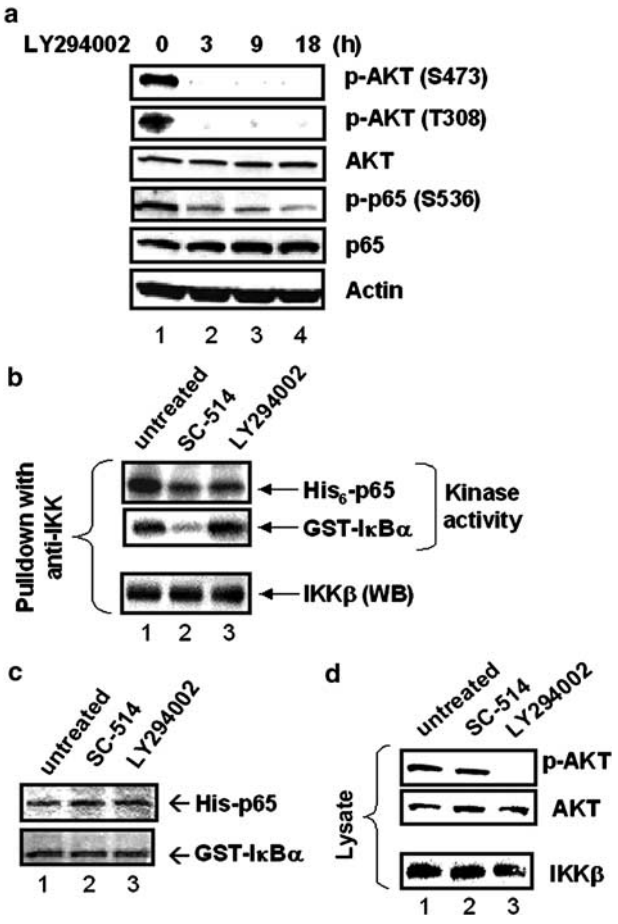

Figure 5 AKT induces IKKβ kinase activity to phosphorylate p65 in HTLV-1-transformed cells. (**a**) C81 cells were treated with LY294002 (20 μM) for 0, 3, 9 or 18 h. Whole cell extracts were prepared and Western blot analysis was performed to detect the expression of phospho-AKT, AKT, phospho-p65 Ser-536 (Cell Signaling), p65 (CT, Upstate) and actin (Santa Cruz) as visualized by chemiluminesence. (**b**) *In vitro* IKK kinase assays were performed with cytoplasmic fraction of HTLV-1-transformed C81 cells. Cells were untreated (lane 1) or treated with SC-514 (lane 2, 50 μM, Calbiochem) or LY294002 (lane 3, 20 μM, Calbiochem) for 18 h and extracts were immunoprecipitated with anti-IKKβ antibody (Santa Cruz). Kinase reaction was performed in kinase buffer with substrate (1 μg), 6× His-p65 (upper panel) or GST-IκBα (middle panel), at 30°C for 30 min. Samples were separated by electrophoresis in 4–20% Tris-glycine gel (Novex) and then kinase activity was quantified on a Phospho-Image. Immunoprecipitates were separated in 4–20% Tris-Glycine gel and analysed with anti-IKKβ. (**c**) Gelcode-stained membrane shows that the same amounts of substrate, 6× His-p65 (left panel) or GST-IκBα (right panel) were added to the reaction mix. (**d**) Western blot analysis was performed with cell lysates, which were untreated or treated with LY294002 or SC-514 for phospho-AKT, AKT and IKKβ

In our previous study, we demonstrated a strong correlation between IKKβ-induced p65 phosphorylation and p53 inhibition (Jeong *et al*., 2005). In view of the observation that AKT kinase activity influences p53 inhibition, we assessed whether AKT is directly linked to IKKβ kinase activity in HTLV-1-transformed cells. Following treatment with the IKKβ-specific inhibitor SC-514 or AKT inhibitor LY294002, cell lysates were prepared, immunoprecipitated with anti-IKKβ antibody, and *in vitro* kinase activity was measured using either GST-IκBα or 6× His-p65 as a substrate. Interestingly, both SC-514 and LY294002 treatments reduced IKKβ kinase activity for the phosphorylation of p65 (Figure 5b, upper panel), suggesting a link between AKT and IKKβ in p65 phosphorylation. In contrast, SC-514 but not LY294002 treatment inhibited phosphorylation of IκBα (Figure 5b, middle panel). Western blot analysis of IKKβ from immunoprecipitates demonstrated that equal amounts of IKKβ were present in each reaction (Figure 5b, bottom panel). This result suggests that IKKβ phosphorylation of IκBα is independent of AKT activity, whereas phosphorylation of p65 is AKT dependent. GelCode staining of the reactants demonstrated that comparable amounts of p65 or IκBα were present in each of the reactions (Figure 5c). Cell lysates were separated by electrophoresis in 4–20% Tris-glycine gel and analysed for phospho-AKT, AKT and IKKβ (Figure 5d). The level of phospho-AKT was decreased by the treatment with LY294002, but not with SC-514. Overall levels of AKT and IKKβ were constant in all reactions. Taken together, the results suggest that the phosphorylation of IκBα and p65 by IKKβ in HTLV-1-transformed cells is regulated through distinct pathways, PI3K/AKT-independent and -dependent, respectively.

LY294002 induces RNA expression of the p53-responsive gene MDM2 in HTLV-1-transformed cells

Since LY294002 treatment abrogated Tax-mediated p53 inhibition in transfection studies, we determined the effect of LY294002 on the expression of the p53-responsive gene *MDM2* in HTLV-1-transformed cells. C81 cells were treated with LY294002 for 0, 6, 12, 18 or 24 h. RNAs were isolated and the relative RNA expression levels were analysed by reverse transcription –polymerase chain reaction (RT–PCR). As shown in Figure 6, MDM2 expression was increased approximately 2.5-fold 6–18 h after treatment with the inhibitor in three independent assays. No increase in RNA synthesis was observed with the GAPDH control. Real-time RT–PCR analysis confirmed the increase of MDM2 mRNA expression by LY294002 (data not shown). Unfortunately, because of low transfection

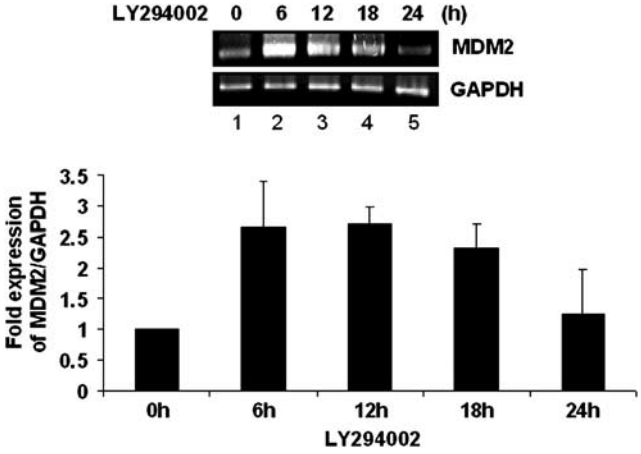

Figure 6 LY294002 treatment increases the expression of p53-responsive *MDM2* in HTLV-1-transformed cells. C81 cells were treated with LY294002 (20 μM) for 0, 6, 12, 18 or 24 h and total RNAs were isolated by RNeasy Mini kit (Qiagen). Reverse transcription (RT)–polymerase chain reaction (PCR) was performed for analysing the RNA expression of MDM2 and GAPDH (upper panel). The graph represents the relative levels of MDM2 RNA expression from three independent experiments. The s.d. for the three experiments is included

efficiency of C81 cells, AKT SiRNA studies could not be performed in HTLV-1-transformed cells.

Blocking AKT in HTLV-1-transformed cells induces cell death and downregulation of the antiapoptotic Bcl-xL

Several assays to analyse cell death were performed to test whether AKT plays a role in promoting survival and repressing cell death in HTLV-1-transformed cells. First, the cytotoxicity of LY294002 in HTLV-1-transformed C81 cells was measured using the LDH release assay. Cells were treated with LY294002 and then incubated for 3, 9, 18 or 24 h. To determine 100% LDH release, an aliquot of the cells was lysed with Triton X-100. The results of these studies demonstrate that in comparison to DMSO-treated controls, lactose dehydrogenase (LDH) release increased with LY294002 treatment in a time-dependent manner (Figure 7a). We next used the Trypan blue dye exclusion assay to determine if the pharmacological blockade of AKT can affect cell death. C81 cells were treated with LY294002 and analysed for cell death up to 72 h. The results of these studies, consistent with the results of the LDH release assay, suggested that LY294002 treatment induced cell death (Figure 7b). No increase in cell death was observed in the DMSO-treated control cells.

Next, we utilized the TUNEL assay as an index of apoptotic cell death. As in the previous experiments, C81 cells were treated with either DMSO or LY294002 for 0, 6, 9, 12, 15 or 24 h. TUNEL-positive cells were measured by flow cytometry. Consistent with the results presented above, we observed a time-dependent increase in the number of TUNEL-positive cells in the presence of LY294002 (Figure 7c). In addition, cell cycle analysis showed that the treatment with LY294002 induced G1 phase arrest of cell cycle as well as apoptosis (Figure 7d and e). Cells were fixed with 70% ethanol, permeabilized and stained with propidium iodide solution. The stained cells were analysed for cell cycle distribution by flow cytometry. LY294002-treated C81 cells increased the percentage of cells in G1 (60% at 18 h and 70% at 24 h) and undergoing apoptosis (20% at 18 h). Lastly, we utilized Western blot analysis to measure the level of NF-κB responsive antiapoptotic genes *Bcl-xL*, *Bcl-2* and *XIAP* (Figure 7f). Of interest, the results demonstrated that the level of Bcl-xL was significantly decreased in response to LY294002 treatment in three independent experiments. In contrast, the expression of Bcl-2 and XIAP were not affected by LY294002 treatment, suggesting a differential regulation of the antiapoptotic proteins. In this regard, Raina *et al*. (2004) reported that the MUC1 transmembrane glycoprotein, which increases the level of phospho-AKT, increases the expression of Bcl-xL but not of Bcl-2. Our studies suggest that Tax may regulate survival of the cells through activation of Bcl-xL through the AKT/NF-κB pathway. LY294002 is not a specific inhibitor for AKT but for PI3K; therefore, we cannot rule out the contribution of other PI3K family members.

Discussion

The AKT pathway plays a major role not only in tumor development but also in the tumor's potential response

Figure 7 LY294002 treatment promotes cell death and correlates with the expression of Bcl-xL in HTLV-1-transformed cells. (**a**) The cytotoxicity of LY294002 was measured by lactose dehydrogenase (LDH) release assay. C81 cells were incubated for 0–24 h with LY294002. The absorbances of the sample were measured at 490 nm (reference wave length was 620 nm) by using OPTImax tunable microplate reader (Molecular Device Corporation). For positive control, cells were incubated in 2% Triton X-100-containing media. Values in a graph are expressed as percentage of cytotoxicity in which positive control is set at 100%. (**b**) Cell death was measured by Trypan blue dye exclusion assay. C81 cells were incubated with LY294002 for indicated time points and cells that took up Trypan blue were counted as dead cells. Error bars were calculated using three independent experiments. (**c**) TUNEL assay was performed by flow cytometry analysis. C81 cells were treated with LY294002 (20 μM) for 0, 6, 9, 12, 15 or 24 h and incubated with terminal deoxynucleotidyl transferase (Oncogene) and FITC-conjugated anti-BrdU monoclonal antibody (Becton Dickinson Bioscience). The values present the percentage of TUNEL-positive cells. Error bars were calculated using three independent experiments. (**d** and **e**) C81 cells were transfected with LY294002 for 0, 6, 12, 15, 18 or 24 h, harvested and fixed in 70% ethanol. Cells were stained with propidium iodide solution and analysed for cell cycle distribution by flow cytometry. The percentage of cells in G1 phase or undergoing apoptosis was determined. (**f**) C81 cells were treated with LY294002 for 0, 3, 9 or 18 h. Cell lysates were prepared and Western blot analysis was performed to detect the expression of Bcl-xL, Bcl-2 (Oncogene) and XIAP (Cell signaling) as visualized by chemiluminesence. The graph represents the relative levels of Bcl-xL protein expression from three independent experiments. The s.d. for the three experiments is included

to cancer treatment (Luo *et al*., 2003; Fresno Vara *et al*., 2004; Parsons, 2004). Active AKT has been detected in more than 50% of human cancers (Gills and Dennis, 2004). In brain, prostate, melanoma, lung and endometrial cancers, AKT activation is increased while phosphatidylinositol phosphate 3′-phosphatase (PTEN), a negative regulator of the AKT pathway, is frequently mutated (Cantley and Neel, 1999). Luo *et al*. (2003). have suggested several therapeutic approaches of targeting the AKT pathway in cancer. In cancer cells, AKT is activated by phosphorylation at Thr-308 of the catalytic domain by phosphoinositide-dependent kinase 1 (PDK-1) and at Ser-473 of C-terminal hydrophobic region by PDK-2 (Scheid and Woodgett, 2003). In this study, overexpression of Tax induced phosphorylation of AKT Ser-473 and Thr-308 and blocking AKT by LY294002 significantly decreased the levels of phospho-AKT Ser-473 and Thr-308 in HTLV-1-transformed cells. In an earlier report, Tax transformation-positive and -negative Rat-1 cell clones were established in which

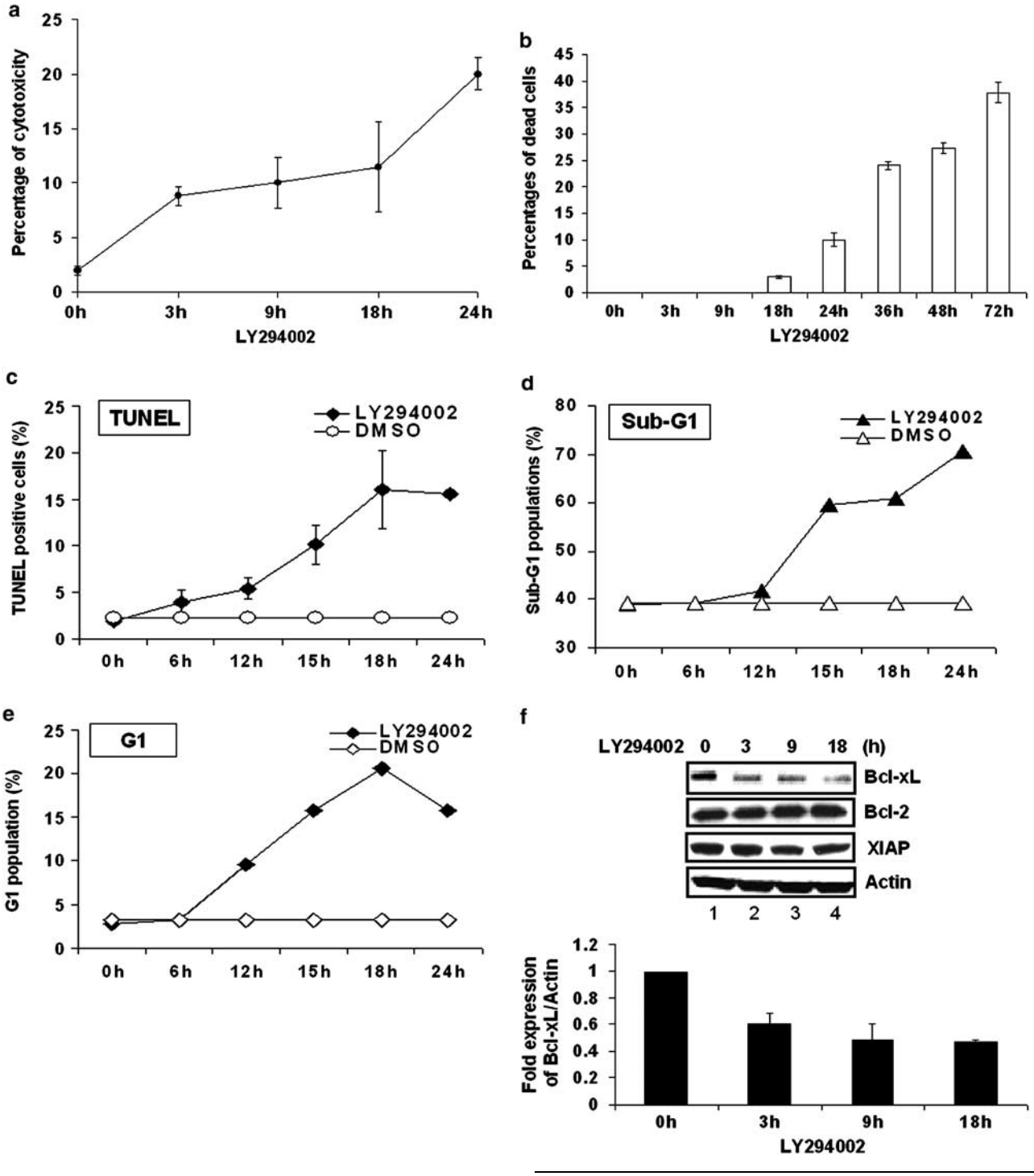

PI3K signal pathway activation was observed to be involved in the cell transformation induced by Tax (Liu *et al*., 2001). Consistent with our results, phosphorylation of AKT Ser-473 was observed in the transformed cells. In the light of the results of these studies, it would be of interest to consider AKT as a molecular target in HTLV-1-transformed ATL cells.

Blocking AKT activity by LY294002 induced cell death and cell cycle arrest in HTLV-1-transformed cells, suggesting that Tax activation of AKT plays a role in survival signaling of HTLV-1-transformed cells. Hovelmann *et al*. (2004). previously demonstrated that AKT increases expression of the antiapoptotic Bcl-2 family member protein Bcl-xL using a constitutively active form of AKT (CA-AKT)-expressing cells. Consistent with these studies, our results showed a decrease in the level of Bcl-xL, but not Bcl-2 or XIAP, by LY294002 treatment in HTLV-1-transformed C81 cells. These data indicate that Tax's ability to protect apoptotic cell death may, in part, be regulated through AKT and Bcl-xL pathways. Numerous studies reported that blocking AKT by LY294002 induces p53-dependent apoptosis and delays onset of the p53 pathway after treatment with drugs, such as cisplatin or mitoxantrone (Ren *et al*., 2003; Hovelmann *et al*., 2004). Our data demonstrated that inhibition of AKT induces p53 transcription activity and apoptosis in HTLV-1 cells. It will be of interest to determine if the two pathways are linked.

In a previous study, we demonstrated that Tax induces the inhibition of p53 transcription activity and IKKβ and p65 phosphorylation at Ser-536 are responsible for the regulation of this pathway (Pise-Masison *et al*., 2000; Jeong *et al*., 2004, 2005). Our present data suggest that AKT lies upstream of IKKβ and is critically involved in the Tax-mediated p53 inhibition pathway. Overexpression of AKT WT, but not the KD mutant, dramatically increased Tax inhibition of p53 in Jurkat T lymphocytes. In addition, blocking AKT with LY294002 impaired p53 inhibition by Tax. Importantly, we showed, directly using AKT SiRNA transfections, that AKT functions to mediate Tax inhibition of p53. p53 acts largely by promoting the transcription of p53-responsive genes, such as *MDM2* (Downward, 2004). In this study, we observed that blocking AKT with LY294002 increased MDM2 expression in HTLV-1-transformed cells. Consistent with the increase in MDM2, we see a slight increase in the level of p53 protein in LY294002-treated cells (data not shown).

AKT-dependent phosphorylation of p65 in HTLV-1-transformed cells is consistent with the finding of Madrid *et al*. (2000) who demonstrated that activated AKT stimulates IKKβ to phosphorylate and activate the transactivation domain (TAD) of p65. Furthermore, Sizemore *et al*. (1999, 2002) demonstrated that PI3K/AKT is important for the phosphorylation and activation of p65 in response to IL-1 and TNF, and that AKT-mediated NF-κB activation required IKK activity. In contrast, Yang *et al*. (2003) demonstrated that the LPS-induced p65 phosphorylation at Ser-536 was independent of the PI3K/AKT signaling pathway. These data suggest that IKK-induced p65 phosphorylation can be regulated by AKT-dependent or -independent pathways, which may result from cell-type differences and NF-κB signaling pathways. Our results demonstrated that LY294002 treatment reduced the level of phospho-p65 Ser-536. Thus, in HTLV-1-transformed cells, Tax activation of AKT is linked to p65 Ser-536 phosphorylation.

In summary, we demonstrate that AKT is activated in HTLV-1-transformed cells and that Tax activation of AKT is linked to three important pathways, which include NF-κB activation, p53 inhibition and cell survival. NF-κB activation requires AKT kinase activity since overexpression of AKT WT, but not the KD mutant, resulted in increased Tax-mediated NF-κB activation. p53 inhibition by Tax is linked, at least in part, to AKT-mediated NF-κB activation. It is important to note, however, that while the NF-κB pathways for transcription activation and p53 inhibition overlap, they are functionally distinct since NF-κB transcription activity is not required for p53 inhibition (Jeong *et al*., 2005). The AKT pathway, because of its central importance to NF-κB activation, p53 inhibition and cell survival, is an attractive target to induce cell death in HTLV-1-transformed cells.

Materials and methods

Cell lines and transfections

HTLV-1-transformed cell lines C81 and T-lymphocytic cell line Jurkat were maintained in RPMI supplemented with 10% fetal calf serum, 2 mM L-glutamine and penicillin/streptomycin. 293T cells were maintained in DMEM supplemented with 10% fetal calf serum, 2 mM L-glutamine and penicillin/streptomycin. Mouse embryo fibroblast (MEF) p65−/− cells were cultured in DMEM medium supplemented with 10% newborn calf serum, 2 mM L-glutamine and penicillin/streptomycin. MEF p65−/− cells were previously described. Jurkat cells were transfected using Superfect transfection reagent (Qiagen) as described by the manufacturer. 293T and MEFs were transfected using Effectene transfection reagent (Qiagen) or Lipofectamine Plus transfection reagent (Invitrogen), respectively, as described by the manufacturer.

Plasmids and luciferase assay

The reporter constructs MDM2-Luc and 4 × NF-κB-Luc, and Tax expression plasmid (pcTax) have been described previously (Pise-Masison *et al*., 2000). RSVp65 expression plasmid was provided by Dr Neil Perkins (Dundee University, UK). AKT WT and KD mutant were provided by Dr Craig Whiteford (National Institutes of Health, Bethesda, MD, USA). For luciferase assay, cell lysates were prepared 24 h after transfection following the Promega Dual Luciferase and Tropix GalactoLight assay kit instructions. MEF p65−/− cells were treated with PI3K/AKT inhibitor LY294002 (Calbiochem) for 1 h before transfection and then replaced with serum-containing media 3 h after transfection. SiRNA oligonucleotides for AKT1 (Dharmacon) and for chloramphenicol acetyltransferase (CAT) (Qiagen) were transfected using RNAifect transfection reagent (Qiagen) 12 h before DNA transfection. All transfections included the control plasmid RSV β-gal to control for transfection efficiency.

Western blot analysis

Cell extracts were prepared by using lysis buffer (50 mM Tris, 120 mM sodium chloride, 5 mM EDTA, 0.5% Noniodet P-40, 50 mM sodium fluoride and 0.2 mM sodium vanadate). The extracts were incubated on ice for 15 min, centrifuged (10 000 *g*) at 4°C for 10 min and supernatants were collected. Protein concentrations were determined by Bradford assay (Bio-Rad), and 50–100 μg was separated by electrophoresis on 4–20% Tris-glycine gels (Novex). The proteins were then transferred to PVDF membranes (Immobilion), analysed for desired antibodies. Anti-p65 and AKT were obtained from Upstate. Anti-phospho-p65 (Ser-536), phospho-AKT (Ser-473), phospho-AKT (Thr-308) and X-chromosome-linked inhibitor of apoptosis protein (XIAP) were purchased from Cell Signaling. Anti-p53 (Ab1), Bcl-xL and Bcl-2 were purchased from Oncogene Research Products. To detect the expression of Tax protein, anti-Tab172 monoclonal antibody was used.

In vitro *IKK kinase assay*

For immunoprecipitation (IP) kinase assay, IKK complexes from cytoplasm were precipitated with anti-IKKβ (Santa Cruz Biotechnologies), followed by treatment with 10 μl of Dynal beads protein G (Dynal Biotech). Immunoprecipitates were washed twice with lysis buffer and twice with kinase buffer (20 mM HEPES, pH 7.6, 20 mM $MgCl_2$, 2 mM dithiothreitol, 20 mM ATP, 20 mM β-glycerolphosphate, 20 mM disodium *p*-nitrophenyl phosphate and 0.1 mM sodium orthovanadate).

Reverse transcription –polymerase chain reaction

Total RNA was isolated using the RNeasy Mini kit (Qiagen). RT–PCR was performed useing the Ambion RT-PCR system, following manufacturers' instructions. Primers were synthesized by Lofstrand and primer sequences are as follows: murine double minute 2 (MDM2) forward, 5′-CAGCTTCGG AACAAGAGACC-3′; reverse, 5′-GTCCGATGATTCC TGCTGAT-3′; glyceraldehydes-3-phosphate dehydrogenase (GAPDH) forward, 5′-GCCAGTGGACTCCACGAC-3′; reverse, 5′-CAACTACATGGTTTACATGTTC-3′. PCR conditions comprised the initial steps at 95°C for 10 min, followed by 30 cycles at 95°C for 1 min, 55°C for 1 min and 72°C for 2 min, and finally at 72°C for 10 min.

Cytotoxicity test by lactose dehydrogenase (LDH) release assay

The assay was performed according to the manufacturer's instructions of the Cytotoxicity Detection kit (Roche). Briefly, cells were collected by centrifugation and culture supernatants were removed carefully. Equal volumes of sample and reaction buffer were added into a 96-well microplate and the reaction mixtures were incubated for 15–30 min at room temperature. For positive control, cells were incubated in 2% Triton X-100 containing RPMI. The absorbance of the sample was measured at 490 nm (reference wave length was 620 nm) by using OPTImax tunable microplate reader (Molecular Devices Corporation).

Trypan blue dye exclusion assay

To measure cell death, cells were stained with 0.4% Trypan blue solution (Quality Biotech) for 5 min. The number of cells that took up Trypan blue were counted as dead cells using a hemocytometer, and expressed as a percentage of the total cell number.

Terminal deoxynucleotidyl transferase (TdT)-mediated dUTP biotin nick end-labeling (TUNEL) assay

C81 cells (10^6 cells) were fixed in suspension for 15 min in 1% methanol-free formaldehyde (Pierce) in PBS, pH 7.4, on ice, centrifuged at 200 *g* for 5 min at 4°C and added to ice-cold ethanol at 75% of final concentration. After centrifugation, cells were incubated with terminal deoxynucleotidyl transferase (Oncogene Research Products) and FITC-conjugated anti-BrdU monoclonal antibody (Becton Dickinson Bioscience) and then analysed by FACScan flow cytometry (Becton Dickinson Bioscience) by counting the percentages of TUNEL-positive cells.

Cell cycle analyses

Cells were harvested and fixed in 70% ethanol. The fixed cells were then stained with propidium iodide (50 μg/ml) after treatment with RNase (5 μg/ml). The stained cells were analysed for DNA content using FACSCalibur (Becton Dickinson Bioscience). Cell cycle fractions were quantified with Cell Quest (Beckton Dickinson Bioscience) or ModFit LT (Verity Software House).

Acknowledgements
We thank members of Dr Brady's laboratory for helpful discussion and the FACS core facility of CCR, NCI and NIH for flow cytometry analysis.

References

Akagi T, Ono H and Shimotohno K. (1995). *Blood*, **86,** 4243–4249.
Bellacosa A, Testa JR, Staal SP and Tsichlis PN. (1991). *Science*, **254,** 274–277.
Cantley LC and Neel BG. (1999). *Proc. Natl. Acad. Sci. USA*, **96,** 4240–4245.
Downward J. (2004). *Semin. Cell Dev. Biol.*, **15,** 177–182.
Dudek H, Datta SR, Franke TF, Birnbaum MJ, Yao R, Cooper GM, Segal RA, Kaplan DR and Greenberg ME. (1997). *Science*, **275,** 661–665.
Fresno Vara JA, Casado E, de Castro J, Cejas P, Belda-Iniesta C and Gonzalez-Baron M. (2004). *Cancer Treat. Rev.*, **30,** 193–204.
Gessain A, Barin F, Vernant JC, Gout O, Maurs L, Calender A and de The G. (1985). *Lancet*, **2,** 407–410.
Gills JJ and Dennis PA. (2004). *Expert. Opin. Invest. Drugs*, **13,** 787–797.
Grassmann R, Dengler C, Muller-Fleckenstein I, Fleckenstein B, McGuire K, Dokhelar MC, Sodroski JG and Haseltine WA. (1989). *Proc. Natl. Acad. Sci. USA*, **86,** 3351–3355.
Hovelmann S, Beckers TL and Schmidt M. (2004). *Br. J. Cancer*, **90,** 2370–2377.
Jeong SJ, Pise-Masison CA, Radonovich MF, Park HU and Brady JN. (2005). *J. Biol. Chem.*, **280,** 10326–10332.
Jeong SJ, Radonovich M, Brady JN and Pise-Masison CA. (2004). *Blood*, **104,** 1490–1497.

Kauffmann-Zeh A, Rodriguez-Viciana P, Ulrich E, Gilbert C, Coffer P, Downward J and Evan G. (1997). *Nature*, **385,** 544–548.
Kulik G, Klippel A and Weber MJ. (1997). *Mol. Cell Biol.*, **17,** 1595–1606.
Levine AJ. (1997). *Cell*, **88,** 323–331.
Liu Y, Wang Y, Yamakuchi M, Masuda S, Tokioka T, Yamaoka S, Maruyama I and Kitajima I. (2001). *Oncogene*, **20,** 2514–2526.
Luo J, Manning BD and Cantley LC. (2003). *Cancer Cell*, **4,** 257–262.
Madrid LV, Wang CY, Guttridge DC, Schottelius AJ, Baldwin Jr AS and Mayo MW. (2000). *Mol. Cell Biol.*, **20,** 1626–1638.
Mayo LD and Donner DB. (2002). *Trends Biochem. Sci.*, **27,** 462–467.
Mochizuki M, Watanabe T, Yamaguchi K, Takatsuki K, Yoshimura K, Shirao M, Nakashima S, Mori S, Araki S and Miyata N. (1992). *Jpn. J. Cancer Res.*, **83,** 236–239.
Nerenberg M, Hinrichs SH, Reynolds RK, Khoury G and Jay G. (1987). *Science*, **237,** 1324–1329.
Nishioka K, Maruyama I, Sato K, Kitajima I, Nakajima Y and Osame M. (1989). *Lancet*, **1,** 441.
Osame M, Usuku K, Izumo S, Ijichi N, Amitani H, Igata A, Matsumoto M and Tara M. (1986). *Lancet*, **1,** 1031–1032.
Ozes ON, Mayo LD, Gustin JA, Pfeffer SR, Pfeffer LM and Donner DB. (1999). *Nature*, **401,** 82–85.
Parsons R. (2004). *Semin. Cell Dev. Biol.*, **15,** 171–176.
Pise-Masison CA, Mahieux R, Jiang H, Ashcroft M, Radonovich M, Duvall J, Guillerm C and Brady JN. (2000). *Mol. Cell Biol.*, **20,** 3377–3386.
Poiesz BJ, Ruscetti FW, Gazdar AF, Bunn PA, Minna JD and Gallo RC. (1980). *Proc. Natl. Acad. Sci. USA*, **77,** 7415–7419.
Raina D, Kharbanda S and Kufe D. (2004). *J. Biol. Chem.*, **279,** 20607–20612.
Ren S, Gao C, Zhang L, Koike K and Tsuchida N. (2003). *Biochem. Biophys. Res. Commun.*, **308,** 120–125.
Scheid MP and Woodgett JR. (2003). *FEBS Lett.*, **546,** 108–112.
Shan X, Czar MJ, Bunnell SC, Liu P, Liu Y, Schwartzberg PL and Wange RL. (2000). *Mol. Cell Biol.*, **20,** 6945–6957.
Sherr CJ. (1998). *Genes Dev.*, **12,** 2984–2991.
Sizemore N, Lerner N, Dombrowski N, Sakurai H and Stark GR. (2002). *J. Biol. Chem.*, **277,** 3863–3869.
Sizemore N, Leung S and Stark GR. (1999). *Mol. Cell Biol.*, **19,** 4798–4805.
Slee EA, O'Connor DJ and Lu X. (2004). *Oncogene*, **23,** 2809–2818.
Songyang Z, Baltimore D, Cantley LC, Kaplan DR and Franke TF. (1997). *Proc. Natl. Acad. Sci. USA*, **94,** 11345–11350.
Staal SP, Hartley JW and Rowe WP. (1977). *Proc. Natl. Acad. Sci. USA*, **74,** 3065–3067.
Tanaka A, Takahashi C, Yamaoka S, Nosaka T, Maki M and Hatanaka M. (1990). *Proc. Natl. Acad. Sci. USA*, **87,** 1071–1075.
Thompson JE and Thompson CB. (2004). *J. Clin. Oncol.*, **22,** 4217–4226.
Vernant JC, Buisson G, Magdeleine J, De Thore J, Jouannelle A, Neisson-Vernant C and Monplaisir N. (1988). *Lancet*, **1,** 177.
Vousden KH and Lu X. (2002). *Nat. Rev. Cancer*, **2,** 594–604.
Vousden KH. (2000). *Cell*, **103,** 691–694.
Yang F, Tang E, Guan K and Wang CY. (2003). *J. Immunol.*, **170,** 5630–5635.
Yoshida M, Miyoshi I and Hinuma Y. (1982). *Proc. Natl. Acad. Sci. USA*, **79,** 2031–2035.